QUANTUM DOTS NANO-PARTICLES FULL FIELD IMAGING WITH OPTICAL SECTIONING AND 3D LOCALIZATION

F. Chasles, B. Dubertret and A.C. Boccara

Laboratoire de Spectroscopie en Lumière Polarisée, UPR A0005 du CNRS, ESPCI,
10 rue Vauquelin, 75213 Paris, France

ABSTRACT

We present in this paper a technique for imaging fluorescent particles based on the axial modulation of the objective's focal plane position. This technique provides full field optical sectioning and can be used to localize the fluorophores in three dimensions. We describe the technique and apply it to image polymer beads filled with quantum dots immobilized in a gel. We show that full field optical sectioning is obtained and that the beads are localized with a precision of 10 nm in the transverse plane and 31 nm in the axial direction.

1. INTRODUCTION

Single-particle detection has evolved within the last 15 years to become a useful tool to address a broad range of questions in the field of physics[1], chemistry[2], biology [3]. Optical methods recently developed allows one to study single nano-objects properties (absorption, emission, ...) and can also provide their position with sub-wavelength precision[4]. While the particle localization in the optical transverse plane is quite straightforward -provided good signal to background ratio[5]- the localization in the third dimension along the optical axis is more delicate. So far, it has been done using total internal reflection microscopy[8], 4-Pi set-up [9] and out of focus microscopy [6, 7]. The latter method, is probably the simplest one to implement without special design, but it is limited because of the noise introduced by out of focus objects.

2. THEORY

Here we present a simple method to achieve both *full field optical sectioning and precise localization* of isolated fluorescent beads whose dimensions are below the objective resolution using a standard epifluorescence microscope and a piezoactuator (PZT) for the objective. The image of a fluorescent object is given by its convolution with the 3D Point Spread Function (PSF). When the object dimensions are small compared to the PSF, its image can be assumed to be the PSF itself. Along the optical axis (denoted z in this letter), for a diffraction limited lens and under paraxial approximation, it can be approximated by :[10]

$$I(u) = I_0 \left(\frac{\sin(u/4)}{u/4} \right)^2 \tag{1}$$

with

$$u = \frac{8\pi}{\lambda} n z \sin^2 \left(\frac{\alpha}{2} \right) \tag{2}$$

In equation 1 and 2, I_0 is the intensity at the geometrical focus, α the semi-aperture angle, λ the wavelength, n the medium index and z the axial distance from the focal plane. Modulation of the the focal plane axial position at a frequency ω induces intensity modulations of the fluorescent signal I at frequencies ω and at higher harmonics. In the focal plane, I_ω is minimum while $I_{2\omega}$ is maximum (see fig.1). Signals at ω and 2ω are extracted using four images P_0, P_1, P_2, P_3 acquired during one modulation period. According to the Discrete Fourier Transform Theory [11], I_ω and $I_{2\omega}$ for a given point of coordinates (x,y) can be written as :

$$I_\omega(z) = \frac{1}{4} \left[(P_0 - P_2) + i \, (P_1 - P_3) \right] \tag{3}$$

$$I_{2\omega}(z) = \frac{1}{4} \left[(P_1 + P_3) - (P_0 + P_2) \right] \tag{4}$$

The phase between the focal plane modulation and the sampling signal is adjusted such that $P_1 = P_3$ (see inset of Fig. 1). With such a choice, I_ω is real and $I_{2\omega}$ is maximal, both can be readily extracted from the set of four images taken during the modulation. Each of our four recorded images corresponds to different focus positions so equations 3 and 4 can be rewritten as:

$$I_\omega(z) = \frac{1}{4} \left[P(z+d) - P(z-d) \right] \tag{5}$$

$$I_{2\omega}(z) = \frac{1}{4} \left[2P(z) - P(z+d) - P(z-d) \right] \tag{6}$$

Where d is the amplitude of modulation. Once the two signals are extracted, the fluorescent particle position can be computed using the ration $I_\omega / I_{2\omega}$. Although several functions could be used to analyse this ratio, we found that the function

$\phi = \arctan\left({}^{I_\omega}/_{I_{2\omega}}\right)$ has the advantage of varying linearly as a function of z around $z = 0$ as shown on figure 2, d) if we use a modulation amplitude d equal to half the Full-Width Half-Maximum (FWHM) of the axial response. By finding the slope of this linear part, we can obtain the precise position of the bead on the optical axis with only four images. We simulated a PSF over 2 μm using equation 1 with a point each 40 nm. I_ω and $I_{2\omega}$ were calculated thanks to equations 5 and 6 with $d = 300$ nm (FWHM=600 nm with the model). Theorical results are presented on figure 2, left.

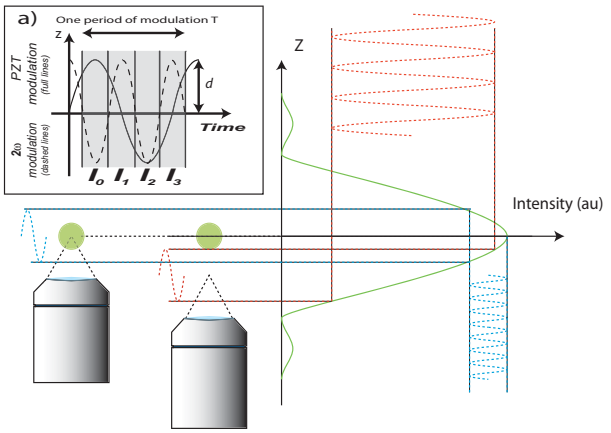

Fig. 1. An axial modulation of the focal plane at the frequency ω induces an intensity modulation of the fluorescence intensity both at ω and 2ω. Inset a) scheme of images acquisition, phase between modulation (continuous line) and acquisition must be correctly adjusted to extract 2ω signal (dashed line)

3. EXPERIMENTAL RESULTS

Experiments were conducted on an Olympus IX71 inverted epifluorescence microscope using a $\times 100$ oil immersion objective (Olympus, NA 1.35) and a mercury lamp for excitation. Axial modulation was realized with a piezoactuator (PiezoJena, PX100). Sample images were recorded with a CCD camera (PCO, PixelFly QE) using an home made software. Synchronization was achieved with two waveform generators (Agilent 33250A) locked in phase. The sample used is made of latex beads (diameter between 100 and 200 nm) filled with Quantum Dots (QD, $\lambda_{em} = 520$ nm) immobilized in an acrylamide gel to avoid any movement. These beads allowed us to obtain SNR higher than 50. As we use a high aperture objective, assumptions done to obtain equation 1 are no longer valid. Actually the system is not aberration free and the PSF along *z-axis* loses its symmetric shape as we move away from the maximum (see figure 2, right a)). Nevertheless, and as shown on figure 2, right, the signals at ω and 2ω are only slightly modified and may still be used to find the position of our beads.

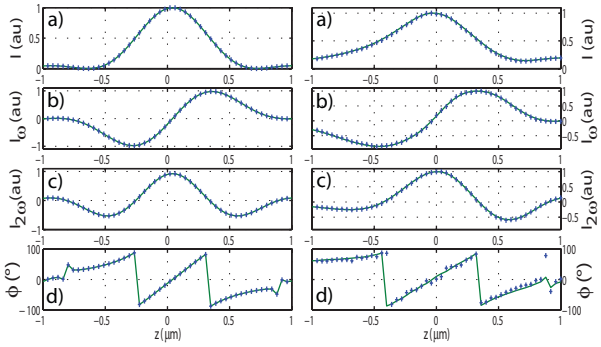

Fig. 2. **Left:** Results of simulations **a)** Intensity along the axis evaluated with equation 1 for an oil immersion objective with a $NA = 1.35$. **b)** I_ω calculated using equation 5 and d=300 nm **c)** $I_{2\omega}$ calculated using equation 6 and d=300 nm **d)** $\phi = \arctan\left(\frac{I_\omega}{I_{2\omega}}\right)$. **Right:** Data from images of fluorescent beads immobilized in a gel. The modulation amplitude is 360 nm. **a)** Intensity along the axis, this is the experimental PSF. Note the tail and the asymmetric shape. **b)** I_ω calculated using equation 3 **c)** $I_{2\omega}$ calculated using equation 4 **d)** ϕ . For all these graphics, signals were measured and calculated each 40 nm (crosses) and we plotted the best curve (continuous lines)

In our experiments we used a sinusoidal modulation. The images $P_0, .., P_4$ are obtained by integration of the fluorescent signal received over a quarter of a modulation period.

We first measured a PSF along z and found a FWHM of $720nm$, larger than the diffraction limited one which can be explained by index mismatch and aberrations[12]. The goal of this measure is to find the modulation amplitude which should be equal to 360 nm in this case. We then measured I_ω and $I_{2\omega}$ using equation 5 and 6 with z varying by steps of 40 nm and d=360 nm, we then deduced ϕ. As shown on figure 2 (right, d)) ϕ exhibits a linear part around the position of the maximum intensity (i.e. the center of the bead) as predicted by our simulations. We fitted this line for different beads and found that the linear dependence of z could be expressed the following way:

$$z = K \times \phi \tag{7}$$

where ϕ is in degree and z in nm. Our measures leaded to $K = 4.2\ nm.deg^{-1}$. To find the coordinates of the beads, we first need to isolate them in the images which is done by applying a simple threshold on the image at 2ω. This threshold eliminates all the objects that are not in the volume of significant modulation. We then calculated the centroid for each bead to obtain their coordinates in the transverse plane and we use the relation between ϕ and z found previously to obtain the axial position of the center of each fluorescent spots. Results are illustrated on figure 3, c).

We evaluated the precision of our measurements by measuring several times the position of a bead without changing

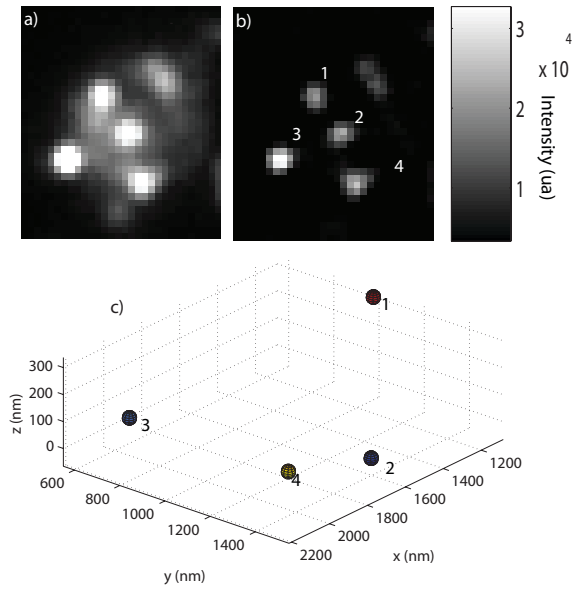

Fig. 3. a) standard epifluorescence image ($2.5 \times 2.9\mu m^2$). b) Image at frequency 2ω without negative values ($2.5 \times 2.9\mu m^2$). c) 3D representation of the samples. Coordinates (x, y, z) of each beads in nm are : bead 1 (1109,1309,312), bead 2 (1534,1343,-41), bead 3 (1893,575,11), bead 4 (2188,1524,185). Uncertainty on x and y is 10nm and 32nm for z.

the focus. For this we took 400 images which correspond to 100 position measurements. We analyzed the beads in the images and found that the experiments gave us the position within 25 nm along the *z-axis*. This variation is due to intensity fluctuations from an image to another. Such a precision on the measured position suggests that there is no drift of the average position of the piezo. The error on the fit on the linear part of ϕ must be taken into account and we finally obtained an uncertainty of 31 nm for the axial positioning. We proceed the same way for lateral positioning and found a precision of 10 nm.

Another interesting feature about this technique is the ability to perform optical sectioning. Indeed, with our modulation technique, a given fluorescent particle is modulated at a frequency 2ω only if the intensity maximum of its axial PSF is modulated. If the modulation occurs above or below the maximum then no signal at 2ω is generated. Consequently, optical sections of the focal plane are obtained as can be seen on Figure 3 $a)$ and $b)$.

After testing the technique with a sinusoidal modulation of the focal plane position, we investigated a stair-case modulation. With such modulation, four images ($P_0 ... P_4$) are taken at four different positions of the piezo. Because of the phase choice between the position modulation of the focal plane and the image acquisition (see eq. 5 and 6), P_0 and P_2 are taken respectively above and below the focal plane while P_1 and P_3 are in focus and identical. This modulation enables us to perform optical sections and to determine the fluorescent particles position either in a given focal plane (as was done previously) or on a stack of images axially separated by half the FWHM (Fig. 4). In the latter case, it is possible once the images stack has been obtained to reconstruct optical cuts at virtually any position (with a resolution depending only on the z spacing between two consecutive images) and to deduce the beads 3D position in the whole volume.

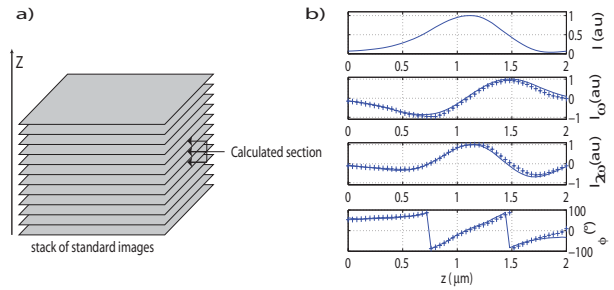

Fig. 4. **right:** stack of images axially separated by half the FWHM. By combining three successive images we can obtain an optical section and precise localization of objects. **left:** Comparison between postprocessing treatment (continuous lines) and real processing (crosses). Images were taken each $40nm$

In conclusion, we have demonstrated a way to achieve precise localization of fluorescent objects with dimensions below objectives resolution with a standard epifluorescence microscope. Combination of sinusoidal modulation (more reliable than an "step by step" motion which is very sensitive to drift) and integration acts like an averaging system providing smoothed signals. This technique should find applications in single particle tracking as it can provide axial position of a molecules within few milliseconds depending on SNR and sensitivity of the camera. It also present the possibility to be used after acquisition

This work has been funded by the Ministère de la Recherche (ACI Jeune Chercheur), the Human Frontier Science Program (Young Investigator Grant) and la Société des Amis de l'E.S.P.C.I. We thank C. Chassenieux for the help in the preparation of the Latex QD beads.

4. COPYRIGHT FORMS

You must include your fully completed, signed IEEE copyright release form when you submit your paper. We **must** have this form before your paper can be published in the proceedings. The copyright form is available as a Word file, a PDF file, and an HTML file. You can also use the form sent with your author kit.

List and number all bibliographical references at the end of the paper. The references can be numbered in alphabetic

order or in order of appearance in the document. When referring to them in the text, type the corresponding reference number in square brackets as shown at the end of this sentence [**?**].

5. REFERENCES

[1] W. E. Moerner, M. Orrit, Sience **283,** 1670 (1999)

[2] L. Kastrup, S. W. Hell, Angew. Chem. Int. Ed. **43,** 6646 (2004)

[3] M. Dahan, S. Levi, C. Luccardini, P. Rostaing, B. Riveau, A. Triller, Science **300,** 442 (2003).

[4] F. Kulzer, M. Orrit, Ann. Rev. Phys. Chem. **55,** 585 (2004).

[5] R. E. Thompson, D. R. Larson, W. W. Webb, Biophys. J. **82,** 2775 (2002).

[6] M. Speidel, A. Jonáš, E.L. Florin, Opt. lett. **28,** 69 (2003).

[7] H. P. Kao, A. S. Verkman, Biophys. J. **67,** 1291 (1994).

[8] R. M. Dickson, D. J. Norris, Y-L Tzeng, W. E. Moerner, Science **274,** 966 (1996).

[9] M. Schimdt, M. Nagorni, S.W. Hell, Rev. sci. Instrum **71,** 2742 (2000).

[10] T. Wilson, C. Sheppard, *Theory and practice of scanning optical microscopy* (1984)

[11] A. V. Oppenheim, R. W. Schafer, *Digital signal processing, chapter 3*

[12] S. Hell, G. Reiner, C. Cremer, E. H. K. Stelzer, J. Microsc. **169,** 391 (1993)